Numerical Computation of Pressure Drop across an Off Supplementary Firing Burner in Heat Recovery Steam Generator

Shervin Karimkashi[1], Mohammad J. Kermani[2], Ahmad Sharifian[3], Javad Hashempour[3]

[1]Department of Mechanical Engineering,
Energy Systems Division, K.N. Toosi University of Technology, Tehran, Iran,

[2]Department of Mechanical Engineering,
Energy Conversion Research Lab., Amirkabir University of Technology, Tehran, Iran,

[3]Computational Engineering and Science Research Centre (CESRC),
University of Southern Queensland, Toowoomba, Australia

Abstract

Combined-gas and steam-turbine power plants have become popular in recent years for distributed power generation and heat production. The optimal thermodynamic and economical design of these plants requires the study of their main components, which are the gas turbine, the steam turbine and the Heat Recovery Steam Generator (HRSG). The HRSG is a heat exchanger that recovers heat from the gas turbine cycle and produces steam and/or hot water, either to be used in a downstream steam cycle or to feed industrial/civil utilities. Some HRSGs include Supplementary Firing (SF) which are additional burners providing additional energy at lower capital costs. However, the supplementary burners cause pressure drops through the duct burner bars which makes the gas turbine to be exhausted at higher pressures. The gas pressure drop should be limited, as previous works show each additional 10 millibars gas pressure drop in the HRSG decreases the gas turbine power output by about 1%. In this work, pressure drop in an off-Supplementary Firing burner of HRSGs has been simulated using two- and three-dimensional models. Simulations indicate that the pressure drop increases with the temperature of the flow entering the burner section. The computational results show very good agreement with semi-empirical results.

Keywords

HRSG, Supplementary Firing, Pressure Drop in an SF, Numerical Computation

Introduction

The use of gas turbines for power generation has increased in recent years and is likely to continue to increase particularly for distributed power and heat production, either for large-size or for small-size plants [9]. HRSG is one of the most used components which recovers heat from the gas turbine cycle and produces steam and/or hot water. The HRSG performances and its matching with other components of the plant are crucial issues for the optimisation of cogeneration and combined cycle plants [11]. Many authors have dealt theoretically with the HRSG thermodynamics optimisation in terms of heat transfer area, heat exchanger tube displacement, steam circulation, mode operation, etc. In this field, interesting models and optimisation strategies are presented in [4] and [5].

Recently, the design of HRSG has also taken advantage of the development and of the extensive use of CFD calculations. In [13], the simulation of an existing entire fired HRSG of the horizontal type has been performed and the results have been compared with experimental data. In particular, emphasis has been given to experimental and numerical pressure drop evaluation through the HRSG and the exhaust duct. CFD analysis of the gas-side flow path of the HRSG as an integral tool in the design process is presented in [11]. The work focuses on how CFD analysis can be used to assess the impact of the gas-side flow on the HRSG performance and identify design modifications. CFD simulations of flow and heat transfer in HRSG of vertical- and horizontal-tube designs were also used in [7], in which two modifications to a HRSG design were compared and the optimal one was studied in details. The study by means of CFD calculations of inlet duct flow distribution of a HRSG in a combined cycle working in partial by-pass mode is presented in [2]. The HRSG/by-pass system was modelled both in maximum open to HRSG position and minimum open to HRSG position and the recirculation flow observed in these two positions. Practical information on the design of the HRSG is instead more difficult to find. In [12], the main characteristics requested by an HRSG when used in single shaft combined cycle power generation systems are described. In [8], the various aspects that have to be analysed for an optimal HRSG design considering the thermodynamic issues as well as the structural and economical ones are depicted.

The HRSG in a combined gas turbine-steam cycle can be designed with a supplementary firing burner placed downstream of the gas turbine in order to increase the tonnage of steam generated. Although with no SF, the efficiency of the combined cycle power plant is higher, but SF allows the plant respond to excessive demands of electrical load [10]. A supplementary fired plant, has the ability to produce more power output during periods of high electricity prices and this, gives it an economic advantage, depending on the demand for the electricity and the duration of high price. To determine the benefits of adding supplementary firing to a plant, any particular application should be analyzed in detail because many variables are involved, such as plant design and regional wholesale electricity prices [1]. Since compressors of gas turbines are constant volume machines, as ambient air temperature increases, turbine air mass flow decreases due to the decreased density of air. This causes drop in the net power out of the gas turbine. This power drop in hot summer seasons can be compensated, using SF in plant. For this purpose a supplementary firing (also called a duct burner in the present study) can be added to enhance the turbine exhaust energy at high ambient temperatures in order to maintain design throttle flow to the steam turbine. Even if only a small duct burner is added to a combined-cycle plant, the economic benefits of SF can be realized in a short payback period, especially on-peak hours of summer months [1].
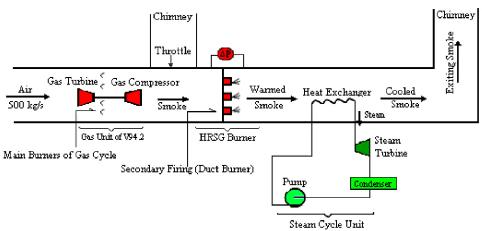
Figure 1. Schematic figure of a combined-cycle

Many researchers have studied SF benefits. When electricity prices are below the cost of production, both unfired and fired plants have a net loss in income. Fired plants have a higher loss because they have a higher cost of production. When electricity prices are higher than the cost of production, both unfired and fired plants have a net gain in income. But fired plants have a higher gain because they have more generating capacity to sell [1].

In this paper, pressure drop in an SF-off HRSG has been computed, using different methods. The importance of this subject is that while supplementary burners (duct burners or secondary burners), are added to the HRSG channel to enhance the capability of the steam cycle, there are some penalties. A pressure drop over the duct burner bars makes the gas turbine to be exhausted at higher pressures, degrading the net power out of the GT unit; see figure 1. In order to achieve the maximum power available from the combined-cycle (GT-steam cycle), the pressure drop within the duct burners should be computed and modified if needed. In this paper, a simplified case of SF-off condition is considered, and the final results have been presented in a table, in different fixed temperatures to make the results closer to the real condition in which combustion raises the air temperature. The working fluid is also taken as air.

Modelling

The CFD modelling in the present study is performed using the software package of Fluent© in 2D and 3D cases and the results are compared with semi-empirical methods assuming a drag coefficient to the duct burner bars. In an HRSG, flow is incompressible and turbulent. The Reynolds number of the flow is well above the critical values and in the order of 10^5. Since an off SF with no combustion has been assumed in this paper, the flow will be isothermal. Standard k-ε method has been chosen in Fluent to solve the problem.

The model developed has been carried out using the commercial Fluent© solver, solving both 2D and 3D models, separately. For grid generation the Gambit© (GAMBIT 2.0.0 by Fluent© Inc.) has been used. The numbers of grids taken are 15,660 cells in the 2D model and 130,000 cells in the 3D case. It takes about 5 minutes for the solver to solve the 2D model and 30 minutes for the 3D model in a PENTIUM4, 1.83GHz CPU and 256 MB of RAM computer. The solutions presented in this paper were converged to residuals of the maximum order of 10^{-3}.

Pressure Drop Computation by Semi-empirical Method

The problem geometry is shown in figure 2 with exact sizes. Unit depth is considered for the HRSG in all of the models because in the 2D model unit depth has been considered automatically by the solver. To compare the results of 2D computations case with the 3D model and the semi-empirical model, the unit depth should also be considered in the later calculations.

We have considered a real case study in a combined-gas and steam-turbine power plant in Iran with gas unit of V94.2 to be solved in this paper. In reality, the inlet mass flow rate is 500 kg/s and the HRSG inlet (inflow) area is taken as 9 m². Since unit depth has been considered for the HRSG in this paper, then the inflow area will be reduced to 3 m² and the mass flow inlet will be considered as (500/3) kg/s, in order to make the final results consistent to the real results.

Semi-empirical relations for finding pressure drop are listed below [3]:

$$V = \frac{\dot{m}}{\rho A_{ch}} \qquad (1)$$

$$Re = \frac{\rho V L}{\mu} \qquad (2)$$

$$D = C_D \times \left(\frac{1}{2}\rho A_p V^2\right) = C_D \times \left(\frac{1}{2}\dot{m}V\right) \qquad (3)$$

$$\Delta P = \frac{D}{A_{ch}} \qquad (4)$$

Using these relations, the pressure drop for ambient temperature of $30\,^\circ$C, has been computed. But before computing the pressure drop, Reynolds number is needed. Pressure drag plays the main role in the present problem with bluff geometry, i.e. the friction drag can be ignored.
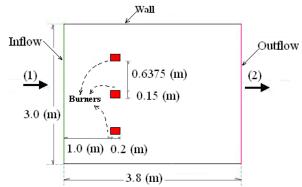

Figure 2. The geometry of the computational domain

At T=30℃ and P=1atm, for L=0.2m (characteristic length of the duct burner body as shown in Figure 2) using equation (1) and equation (2) the Reynolds (Re) number is about 6.0×10^5. For cuboids we take C_D=2.0 if $Re \geq 10^4$ [6]. To calculate the pressure drop across the burners, drag force (D) should be calculated using equation (3) first. The pressure drop will be 397.6 Pa based on equation (4) or 0.392% (considering P_1=1atm=101325Pascal).

Screening Modelling Results

The results presented here are for the temperature of 30˚C. The results at other higher temperatures are not shown for the space limitations. However the summary of the results at other fixed temperatures (isothermal computations) are presented in table1. In fact, Re and D have been altered for each case. As it is not a heat transfer computation, there is no need for any correlations.

Figure 3a shows the contours of velocity magnitudes for the 3D model at the middle depth station. As shown in this figure, there are wake regions behind the bluff geometry of the burners, where velocity magnitudes is at the lowest value right behind the burner (dark-blue color) that gradually increase by diffusion mechanism, as there are entrainments of the flow into the wake. The stagnations regions in front of the burners are also shown by green color. There are similar trends in 2D and 3D computations.

Figure 3b shows the velocity vectors at station O-O upstream of the burner and various stations downstream of the burners for 2D-case. The diffusion process is clearly shown in this figure. The velocity vectors are shown in these locations: (The burners are positioned at x=0). It is clear that turbulent viscosity is the main reason of velocity uniformity.

  O-O section (inflow) at x=-1.2 located upstream of the burner.
  A-A section: x=0.2 located downstream of the burner.
  B-B section: x=1.1 located downstream of the burner.
  C-C section: x=1.8 located downstream of the burner.

Figure 3c shows the stream-wise velocity component profiles in different sections for 2D-case. The horizontal axis shows the positions in the channel and is assumed to be in direction of the inflow section. As shown here the velocity right on the burners (the three black lines in the figure) are zero- due to the no slip condition. At the inflow section the velocity profile is uniform, and locations downstream of the burners, as the station is distanced from the burners, the profile gradually reverts toward the uniform profile.

Figure 4a shows the contour plots of the static pressures. As noted in this figure, the static pressure is at the highest values in front of the burners (approaching to stagnations values).

Figure 4b shows the static pressure profiles in different sections. The horizontal axis shows the positions in the channel and is assumed to be in direction of the inflow section.

Table1 summarizes the results obtained by numerical computation of 2D and 3D cases and semi-empirical methods.

In the case of 2D and 3D, the pressure drops were calculated using the mean inlet and outlet pressures.

From this table, the pressure drop ratio increases with temperature. It is obvious that as the temperature rises, the density of flue gases decreases. Considering equation (1) and equation (3), simultaneously, it is clear that as the density (ρ) decreases the drag force (D) increases and this will lead to the pressure drop increment based on equation (4). It should be noted that because we have only changed the temperature, the mass flow in each run doesn't change and remains as before. Simply, at the inflow boundary we have set the mass flow value.

Also shown in this table is that numerical results (both 2D and 3D), verify semi-empirical results. In fact very good agreement between the results of different methods has been obtained.
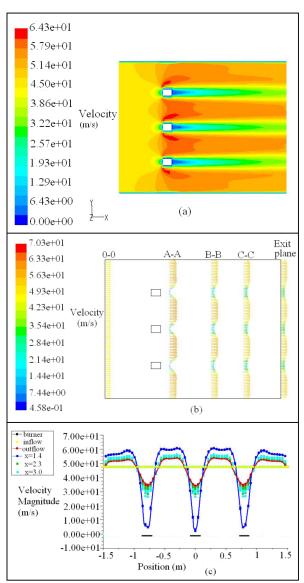

Figure 3. (a) Mean velocity magnitude at the middle depth plane. (b) Mean velocity vectors at different sections for the 2D case. (c) Mean velocity magnitude profiles in different sections in the model, showing how does the mean velocity diffuses gradually, in front of the burners (burners are positioned at x=0)

case	Temperature (℃)	%$\frac{\Delta P}{P_1}$ (semi-empirical)	%$\frac{\Delta P}{P_1}$ (2D model)	%$\frac{\Delta P}{P_1}$ (3D model)
1	30	0.392	0.431	0.415
2	100	0.495	0.531	0.494
3	200	0.622	0.660	0.622
4	300	0.750	0.798	0.752
5	400	0.881	0.943	0.899
6	500	1.012	1.073	1.014
7	600	1.152	1.211	1.141

Table 1. Pressure drop percentages in the HRSG channel in several fixed temperatures using different methods.
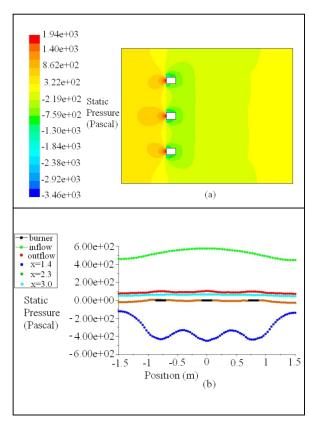
Figure 4. (a) Static pressure contours. (b) Static pressure profiles in different sections (burners are positioned at x=0)

Conclusions

The implementation of SF within the system in one hand increases the rate of steam production in the steam cycle. As a drawback it increases the exit pressure of the turbine that in turn reduces the power output of the gas turbine unit. Therefore, a thorough study of the cost and benefit of the plan is required to give a firm answer on the net amount of performance enhancement of the system.

In this paper, pressure drop in a supplementary firing (SF)-off of Heat Recovery Steam Generator (HRSG) has been computed. The problem is in the case of an off supplementary burner under isothermal assumption at several temperatures. This is a justifiable assumption as there is no combustion in the present SF-off study. These calculations of pressure drop in a Supplementary Firing -Off in a HRSG are performed using numerical method with both 2D and 3D models in order to check on the accuracy of the semi-empirical relations of semi-empirical methods. That is the drag forces on the burner gas delivery bars are obtained, using drag coefficient then the pressure drop over the bars are computed. All the results agree well with each other and numerical computations of pressure drop confirm the results predicted by empirical formulas. Also, all the results show that as the temperature of inflow increase; the ratio of the pressure drop also increases.

To elaborate on the physics of the flow, detailed results of the velocity and static pressure contours and profiles are shown at several stations along the flow as well.

Nomenclature

V	Speed
$\dot{m}$	Mass Flow Rate
ρ	Density
A_{ch}	Channel Inlet Area
D	Drag Force
D_p	Pressure Drag Force
C_D	Pressure Drag Coefficient
A_p	Projected Area
Re	Reynolds Number
L	Characteristic Length of Body
μ	Dynamic Viscosity
ΔP	Static Pressure Drop
T	Static Temprature
P	Static Pressure

References

[1] Backlund J. & Froemming J., *Thermal & Economic Analysis of Supplementary Firing Large Combined Cycle Plants,* Technical Report Coen Company Inc, 2000.

[2] Bell M.B. & Nitzken J.A., *Controlling Steam Production in Heat Recovery Steam Generators for Combined Cycle and Enhanced Oil Recovery Operations*, Technical Report Coen Company Inc, 2003.

[3] Munson B.R., Young D.F. & Okiishi T.H., *Fundamentals of Fluid Mechanics,* John Wiley& Sons, 1998.

[4] Franco A. & Giannini N., A General Method for the Optimum Design of Heat Recovery Steam Generators, *Energy*, **31**, 2006, 3342–3361.

[5] Franco A. & Russo A., Combined Cycle Plant Efficiency Increase Based on the Optimization of the Heat Recovery Steam Generator Operating Parameters, *Int. J. Therm. Sci.,* **41**, 2002, 843–859.

[6] White F.M., *Fluid mechanics*, WCB/Mc Graw-Hill, 1999.

[7] Hegde N., Han I., Lee T.W., & Roy R.P., Flow and Heat Transfer in Heat Recovery Steam Generators, *J. Energy Res. Tech.*, **129(3)**, 2007, 232–242.

[8] Nestianu D., Larson T., Lynch L. & Zachary J., Vertical or Horizontal? An EPC Contractor's Angle, *Modern Power Syst.*, **23(3)**, 2003, 19–22.

[9] Pilavachi M., Power Generation with Gas Turbine Systems and Combined Heat and Power, *Appl. Therm. Eng.,* **20**, 2000, 1421–1429.

[10] Starr F., *Background to the Design of HRSG Systems and Implications for CCGT Plant Cycling*, European Technology Development, Surrey, UK, 2003.

[11] Vytla V.V., & Huang G., *CFD Modeling of Heat Recovery Steam Generators using Fluent,* 30th annual dayton-cincinnati aerospace science symposium; 2005.

[12] Tomlinson L.O. & Mc Cullough S., *Single-shaft Combined-Cycle Power Generation Systems*, Technical Report No. GER-3767, GE Power Systems, 1996.

[13] Torresi M., Saponaro A., Camporeale S.M. & Fortunato B., *CFD Analysis of the Flow through Tube Banks of HRSG*, ASME Paper GT2008-51300, 2008.

[14] Zachary J.J., *Strategies for Integration of Advanced Gas and Steam Turbines in Power Generation Applications*, ASME Paper GT2007-27978, 2007.